Asociación Argentina
de Mecánica Computacional

Mecánica Computacional Vol XXXIV, págs. 151-161 (artículo completo)
Sebastián Giusti, Martín Pucheta y Mario Storti (Eds.)
Córdoba, 8-11 Noviembre 2016

FRAGILITY CURVES OF WOOD UTILITY POLES UNDER STOCHASTIC WIND LOAD WITH MATERIAL UNCERTAIN PROPERTIES

Laura V. González de Paz[a,b], **Diego A. García**[a,b,c] **and Marta B. Rosales**[a,b]

[a]*Department of Engineering, Universidad Nacional del Sur, Bahía Blanca, Argentina.*

[b]*CONICET, Argentina*

Keywords: Wood poles, fragility curves, stochastic wind load, uncertain material properties.

Abstract. Wood utility poles are simple structures used in power networks. Wind loads are one of the main loads and can cause damage. Also, due to the construction procedure and the natural origin of the material, the geometrical dimensions and the material properties usually exhibit variability. The fragility curves are a useful tool to evaluate the failure probability of the poles for a defined failure mode. In this study, displacements are evaluated such that a percentage of damage is found for each wind velocity, and the dynamic behavior of Argentinean *Eucalyptus grandis* wood poles with uncertain material properties is analyzed, giving place to the fragility curves. The stochastic wind velocity field is derived using the Spectral Representation Method (SRM), considering temporal and spatial correlations. Then, the wind load is obtained under the considerations of the Argentinean standard CIRSOC 102. Furthermore, the lengthwise variability of the modulus of Elasticity is simulated through two probabilistic material models: as a random variable and as a random field through the Non Gaussian Karhunen-Loève Expansion . Results are numerically approximated by the Finite Element Method (FEM). Statistics of the response are obtained by means of Monte Carlo Simulations (MCS) with a previous convergence study to determine the acceptable number of realizations. Fragility curves for the probabilistic material models under stochastic wind loads are obtained and compared to assess the uncertainty of the material properties in the structural response.

1 INTRODUCTION

Wood utility poles are simple structures used in power networks. Since they appear in large numbers, their failure can make a significant impact on custom's reliability as well as economic consequences. Uncertainty is the lack of knowledge about a quantity. The probability of structural failure is a function of both uncertainty in the capacity and uncertainty in the demand. The capacity of a structure to withstand a load is a function of its geometry and material properties. Although these quantities can be considered fixed, sometimes and despite the quality process of fabrication or due to the natural origin of materials, uncertainties in their values are unavoidable. Among the existing tools, fragility curves can be useful to represent the probability of failure given a failure mode and a range of loads. In particular, it is a mean to evaluate the behavior of structural systems. A study on the action of wind on industrial steel structures is reported in Palencia et al. (2008) which includes a wide inventory of usual typologies. Fragility curves of the complete structure as well as its components are obtained. *Eucalyptus grandis* is a wood extensively used in Argentina for structural purposes, in particular for utility poles. Experimental studies are usually done to assess its properties and behavior Piter et al. (2004) and more recently, computational approaches are reported García et al. (2015). An experimental assessment of *Eucalyptus grandis* wood poles is contained in Torrán et al. (2009). Wind loads are one of the main causes of damage in this type of structures. The fluctuating wind component is obtained through the Spectral Representation Method (SRM) starting from a given Power Spectral Density Function (PSDF). The temporal and spatial correlations are taken into account by finding the cross-spectrum and introducing a coherence function (Shinozuka and Deodatis, 1991). The method yields a temporal record of the fluctuating wind velocity for each point along the pole height. Combined with the standard recommendations, the fluctuating wind pressure is derived. This method was employed in the dynamic study of a guyed mast and tall buildings (Ballaben and Rosales, 2012; Castro et al., 2015).

The dynamic behavior of Argentinean *Eucalyptus grandis* wood poles with uncertain material properties under stochastic wind load is analyzed. The uncertain material properties are given by the variability of the Modulus of Elasticity (MOE) simulated by two probabilistic material models. In the first one (Unif-model), the value of MOE for the whole pole, is simulated as a random variable through a gamma Probability Density Function (PDF) obtained from the application of the Principle of Maximum Entropy (PME). In the second model (KL-model), the lengthwise variability is simulated with a random field through a Non Gaussian Karhunen-Loève Expansion (NGKLE) with an exponential correlation function (Mulani, 2006) and a gamma marginal distribution. A third model with a homogeneous deterministic MOE is used as a reference.

The fragility curves are obtained from three material models for a given failure mode. Then, they are compared among them. Results are numerically approximated by the Finite Element Method (FEM). Statistics of the response are obtained by means of Monte Carlo Simulations (MCS) with a previous convergence study carried out in order to determine the acceptable number of realizations. The model is discretized using the Finite Element Method (FEM).

2 MODEL DESCRIPTION

2.1 Stochastic wind load

In order to calculate the dynamic stochastic wind load (in the time domain), it is necessary to recreate a temporal record. This record is composed of two contributions: the first one is a fluctuating random variable with the position and time and the second component is a

deterministic mean value with position variation. The fluctuating wind velocity is obtained by the application of Spectral Representation Method (SRM) proposed by Shinozuka and Deodatis (1991). The method starts from a Power Spectral Density Function (PSDF) and a coherence function, to be chosen in accordance with the type of problem to be simulated. Then, the random signals are created as a superposition of harmonic functions with a random phase angle, weighed by coefficients that represent the importance of the value of frequency within the spectrum and the spatial correlation. Following the methodology developed in the reference work, a set of *m* gaussian stationary random processes $f_j^0(t), j = 1, 2, ...m$, with zero mean, $E[f_j^0(t)] = 0$, with a given cross spectral density matrix $S_0(\omega)$ where $S_{jk}^0(\omega) = F[R_{jk(\tau)^0}]$ are considered. $F[\ ]$ represents the Fourier Transform operator and $R_{jk}^0(\tau)$ is the cross-correlation function $(j \neq k)$ or the autocorrelation function $(j = k)$. This matrix verifies $R_{jk}^0(\tau) = R_{jk}^0(-\tau)$ and then, $S^0(\omega)$ is a Hermitian and definite positive matrix. If the lower triangular matrix $H(\omega)$ is defined as a matrix whose Fourier transform exists, the relationship is

$$S^0(\omega) = H(\omega)\bar{H}^T(\omega) \tag{1}$$

where the bar stands for complex conjugate and the superscript T its transpose. The $F_j^0(t)$ process can be simulated by the following Shinozuka & Jan series:

$$f_j(t) = \sum_{k=1}^{3}\sum_{n=1}^{N}|H_{jk}(\omega_n)\mid \sqrt{2\Delta\omega}\cos[\hat{\omega}_n t + \theta_{kj}(\omega_n) + \Phi_{kn}] \tag{2}$$

where $\Delta\omega$ is the frequency interval with which the PSDF is discretized, $\omega_n = \Delta\omega(n-1)$, $\hat{\omega}_n = \omega_n + \psi_{kn}\Delta\omega$, ψ_{kn} is a random value uniformly distributed between 0 and 1, N is the amount of frequency ranges and, Φ_{kn} are the random independent phase angles uniformly distributed between 0 and 2π. If the values S_{jk} are all real, then the $\Theta_{jk}(\omega_n)$ are equal to zero. The decomposition represented by Eq.1 will be found by means of the *Cholesky Decomposition* of the spectral density matrix. The SRM requires of the implementation of different steps. The first one is the adoption of a Power Spectral Density Function (PSDF) and a coherence function. In this case, the PSDF suggested by Davenport is used (Dyrbye and Hansen (1996)):

$$R_N(z,\omega) = \frac{\omega S(z,\omega)}{\sigma^2(z)]} = \frac{2}{3}\frac{f_L^2}{(1+f_L^2)^{4/3}} \tag{3}$$

where ω is the frequency in Hz, σ is the standard deviation and f_L is the non-dimensional frequency:

$$f_L = \omega\frac{L_u}{U(z)} \tag{4}$$

L_u is the length scale of turbulence (1200 m in Davenport's PSDF) and $U(z)$ is the wind mean velocity at height z. The expression for $U(z)$ correspond to the potential law adopted by the Argentinian stardard CIRSOC 102 (2005)

$$U(z) = 2.01V(z/z_g)^{2/\alpha} \tag{5}$$

where V is the nominal wind velocity which, together with z_g and α, are values given by the standard code depending on the characteristics of the structure location.

Then, the assumed coherence function is

$$Coh(z_i, z_j, \omega) = \exp\left\{-2\omega\frac{C_z \mid z_i - z_j \mid}{U(z_i) + u(z_j)}\right\} \tag{6}$$

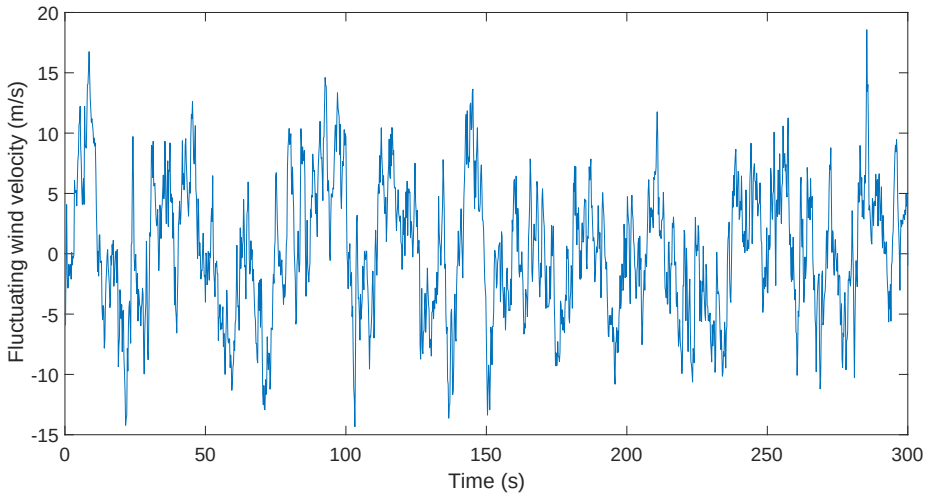

Figure 1: Temporal record of the fluctuating wind velocity component at the middle of the pole height generated through the SRM.

where z_i and z_j are the heights of two given points of the pole. Then, each S_{ij} of the $S(\omega)$ matrix, for a given value of frequency can be calculated as

$$S_{ij}(z_i, z_j, \omega) = \sqrt{S(z_i, \omega) S(z_j, \omega)}\; Coh(z_i, z_j, \omega) \tag{7}$$

Following this procedure, each value $S_{ij}(z_i, z_j, \omega)$ will be calculated, and then, for each frequency ω $H(\omega)$ matrices will be found. Finally, it is possible to construct the temporal series given by

$$u(z_j, t) = \sum_{k=1}^{m} \sum_{n=1}^{N} H_{jk}(\omega_n) \sqrt{2\Delta\omega}\, \cos[2\pi \hat{\omega}_n t + \Phi_{kn}]. \tag{8}$$

The data for the model construction is reported in Table 1. Figure 2.1 shows one of the records generated by this method.

In order to verify the simulated wind register obtained from the model, the PSDF of a register calculated for a given point in the height of the pole is compared with the Davenport'spectrum obtained for the same point. The comparison is depicted in Figure 2.

Table 1: Adopted values employed in the calculation of the time dependent velocity field.

Coefficients	σ^2	L_u	C_z	ω_c	$\Delta\omega$	t	Δt	N	m
Value	38.77	1200 m	11.5	2.5Hz	0.004 Hz	300 s	0.2 s	625	12

When the fluctuating component of the wind speed has been determined, the Argentinean Standard CIRSOC 102 (2005), with some modifications carried out in order to take into account the dynamics of the wind, is employed in the calculation of the wind load. This standard defines the transversal wind force F as:

$$F = q_z\, G C_f A_f \tag{9}$$

where G is the gust-effect factor, C_f is the force coefficient which includes the effect of the shape of the structure, Af is the projected area normal to the wind. q_z is the dynamic velocity pressure evaluated at height z of the structure:

$$q_z = 0.613\, k_z\, k_{zt}\, k_d\, V^2 I \tag{10}$$

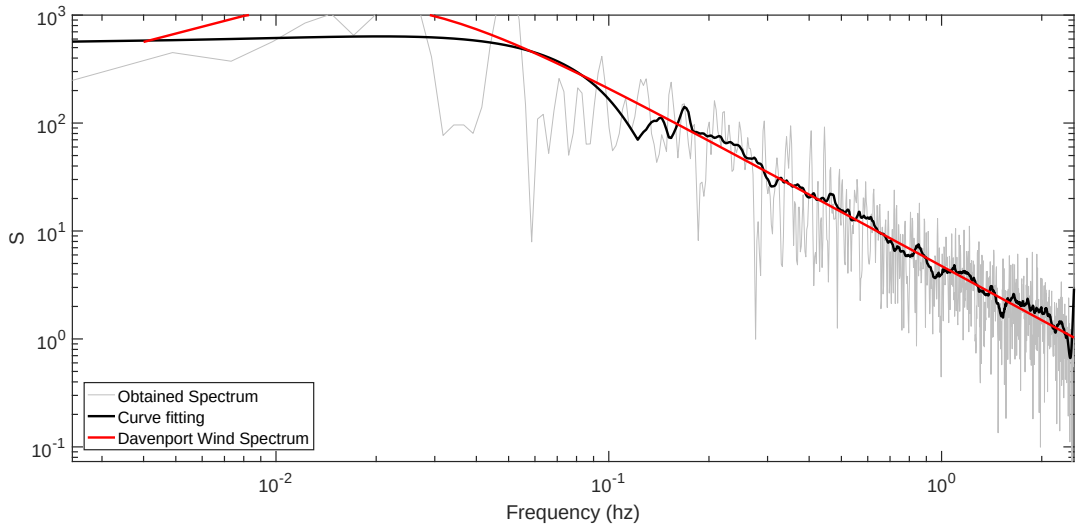

Figure 2: Comparison between theoretical spectrum wind speed (Davenport'spectrum) and the signals generated through the SRM.

where k_z is the dynamic pressure exposure coefficient, k_{zt} is the topographic factor, k_d is the wind directionality factor, V is the basic wind speed and I is the importance factor. k_z is a function of the elevation z and the exposure category that described the ground surface roughness using information about the natural topography, vegetation and constructed facilities in the vicinity of the structure of interest. This parameter can be obtained from the following equation:

$$k_z = 2.01 \left(\frac{max(5\,m, z)}{z_g} \right)^{\frac{2}{\alpha}}, z \leq z_g \tag{11}$$

z_g and α are coefficients obtained according to the exposure category and they are tabulated in the standard.

For the determination of the fluctuating component of the wind velocity, the expression $V\,k_z = U(z)$ was used. Then, the Equation 10 becomes

$$\bar{q}_z = 0.613\,k_{zt}\,k_d(U(z) + u(z))V\,I \tag{12}$$

ant the Equation 9 results:

$$F = \bar{q}_z\,GC_fA_f \tag{13}$$

Table 2 shows the adopted values for the mentioned coefficients.

Table 2: Coefficients employed in the determination of the wind load according to CIRSOC 102 (2005).

Coefficients	G	C_f	I	k_d	k_{zt}	α	z_g
Value	0.85	2.0	1	0.85	1	9.5	274 m

2.2 Structural model

The structure under study is a *Eucalyptus grandis* pole which is a vertical column with variable cross-section (the diameter varies linearly) embedded in the soil (Figure 3). The structural model is a beam clamped at the ground line subjected to wind load. The wind action is

found using the method explained before, and the wood properties parameters and the geometric quantities (height and ground and top diameters) were obtained from Torrán et al. (2009). The geometric quantities are depicted in Table 3.

The MOE will be represented through its mean value in a deterministic case, as a random variable or as a random field, depending on the studied case. The MOE is constant along the pole length in the first two cases (deterministic and random variable).

Table 3: Geometric Data Torrán et al. (2009)

Height	ground line diameter	top diameter
11.975 m	0.262 m	0.191 m

Damping in timber material is considered random with a uniform distribution, assuming values between 1% to 3% of the critical damping c_c. The mass is considered as a deterministic value equal to 707 kg/m^3, corresponding to the mean value presented in Torrán et al. (2009) for a mean moisture content of 45%.

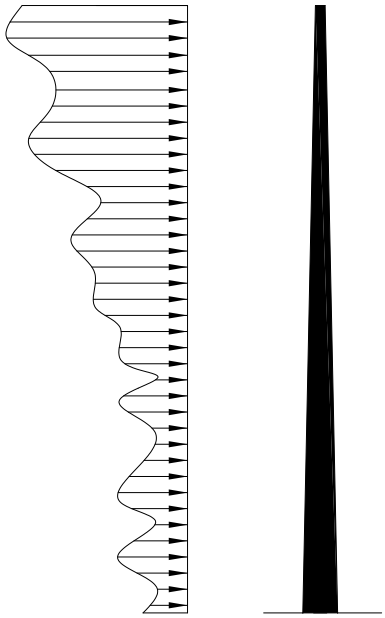

Figure 3: Structural scheme of pole and wind load.

2.2.1 MOE as a random variable

The PDF of the MOE is obtained from the application of the PME. A statistical concept of entropy was introduced by Shannon (1948). PME states that, subjected to known constrains, the PDF which best represents the current state of knowledge is the one with largest entropy. The measure of uncertainties of a continuous random variable X is defined by the following expression

$$S(f_X) = -\int_D f_X(x) ln(f_X(x)) dx, \tag{14}$$

in which f_X stands for the PDF of the random variable X and D is its domain. The domain of the MOE is real and positive and its second moment is bounded. Thus, the stochastic variable MOE will be represented by a gamma PDF with a and b, shape and scale parameters, respectively. Also, $\mu_{MOE} = ab$ and $\sigma^2_{MOE} = ab^2$, where μ_{MOE} is the mean value and σ^2_{MOE} is the variance, given values in this study. The MOE parameters used to make the model are 10.935×10^9 N/m^2 for the mean and 14 % for the Coefficient of Variation (COV) (Torrán et al., 2009).

$$f(H \mid a, b) = \frac{1}{b^a \Gamma(a)} H^{a-1} e^{-\frac{H}{b}}. \tag{15}$$

2.2.2 Non-Gaussian Karhunen-Loève Expansion

The non-Gaussian Karhunen-Loève Expansion (KLE) is applied to simulate the MOE random field. The KLE of the random field of the MOE writes

$$E(x, \theta) = \overline{E}(x) + \sum_{i=1}^{\infty} \sqrt{\lambda_i} \xi_i(\theta) f_i(x), \tag{16}$$

in which λ_i and $f_i(x)$ are the eigenvalues and eigenfunctions of the covariance function $C(x_1, x_2)$, respectively. The parameter ξ_i is a set of uncorrelated random variables. Following the work of Mulani (2006), the non-linear transformation method is applied to obtain KLE basis random variables $\xi_i(\theta)$ of a non-Gaussian process. For the practical implementation, the series are approximated by a finite number of terms M.

3 STUDY CASES

In order to perform the uncertainty quantification, due to the stochastic modeling of the wind load and the MOE, three cases are studied, all of them with stochastic wind load:

- Case 1 (C1): the value of the MOE for the whole pole is considered deterministic and equal to the mean value presented in Torrán et al. (2009).
- Case 2 (C2): the value of the MOE for the whole pole is simulated as a random variable through a gamma PDF.
- Case 3 (C3): the lengthwise variability of the MOE is represented with a random field through a Non Gaussian Karhunen-Loève Expansion with an exponential correlation function and a gamma marginal PDF. After a convergence analysis it is concluded that 30 KL terms are sufficient.

In all cases, the failure of pole is assumed when the demand (displacement on the pole top) S is larger or equal to a given limit (maximum displacement allowed for this structural type) R, *i.e.* the probability of failure can be written as

$$p_f = P(R \leq S) \tag{17}$$

or, in general

$$p_f = P[G(R, S) \leq 0] \tag{18}$$

where $G(\cdot)$ is known as the 'limit state function' and the probability of failure is identical with the limit state violation. In the present study, this limit is set when the displacement in top of the pole (demand S) is equal or larger to a maximum displacement allowed for this structural type of $R = H/100$ (CIRSOC 601, 2011).

4 RESULTS

The structural deterministic problem governed by the Bernoulli-Euler beam equation is solved with a finite element discretization through FlexPDE, PDE (2014) software. After a convergence analysis, a number of 30 quadratic elements with three nodes were used in the FEM model. A Monte Carlo method is used to perform the realizations within the Matlab environment with a number of 600 simulations for each case. Figure 4 shows the results of the analysis made for each study case (C1-C3). In Figure 4(a), the fragility curves (FCs) obtained for each case are presented. All FCs show their failure velocity range around a mean value where the curves intersected. The FC derived for C2 case is the most widespread. For wind velocity lower than the intersection zone, the C2 model leads to higher failure probability.

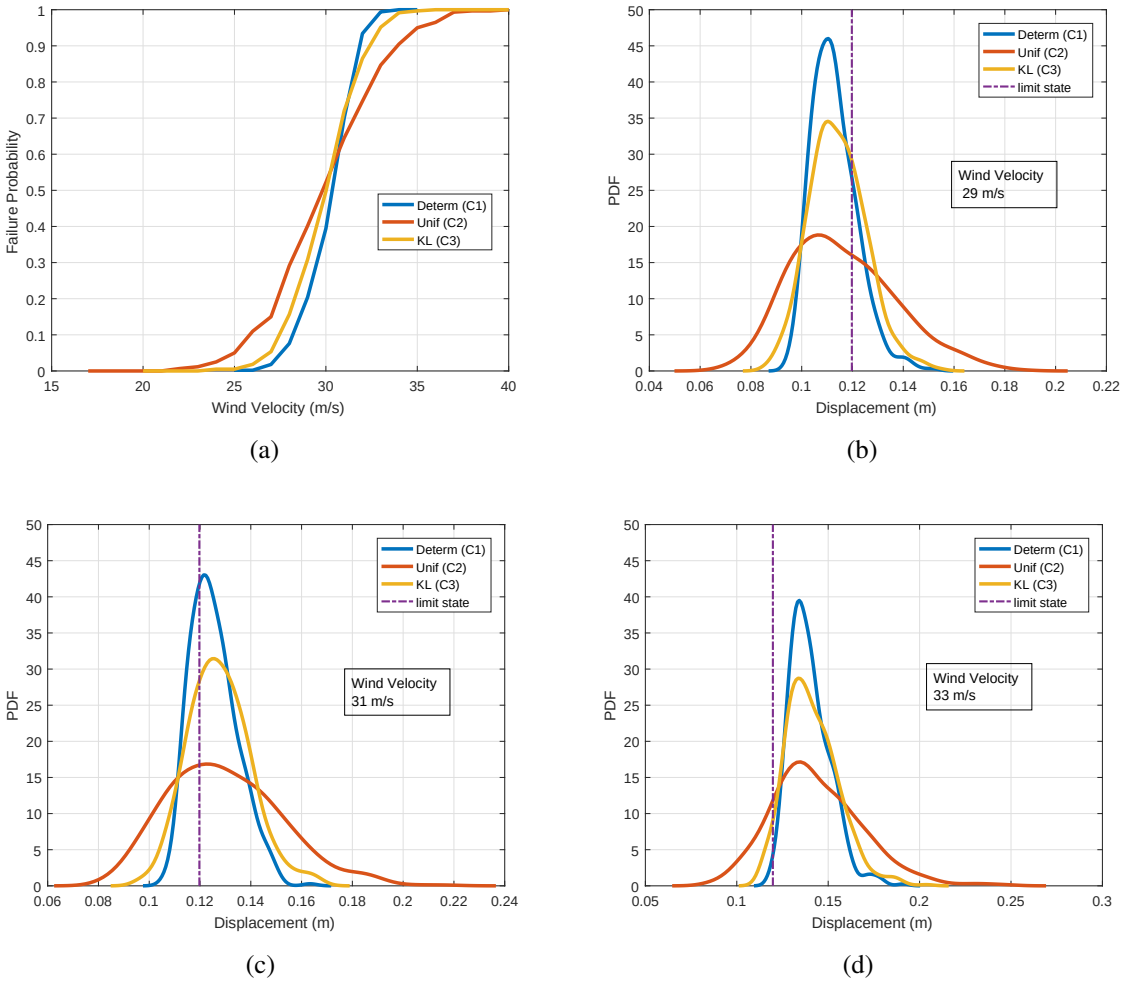

Figure 4: Top displacement of the pole. Three study cases. a) Fragility Curves; b) PDF for a wind velocity V = 29 m/s; c) PDF for a wind velocity V = 31 m/s; d) PDF for a wind velocity V = 33 m/s.

Between the probabilistic material models (C2-C3), the FC derived from C3 exhibits the highest slope than the FC obtained from C2 (probabilistic material models) and a smaller range of failure. It is observed that this curve is closer to the C1 FC (deterministic). Figure 4(b-d) depicts the PDF of the displacements at the pole top for the following wind velocities: 29 m/s (at the left of the intersection zone), 31 m/s (within the intersection zone) and 33 m/s (at the right of the intersection zone). The displacement value adopted as "limit state" is indicated with

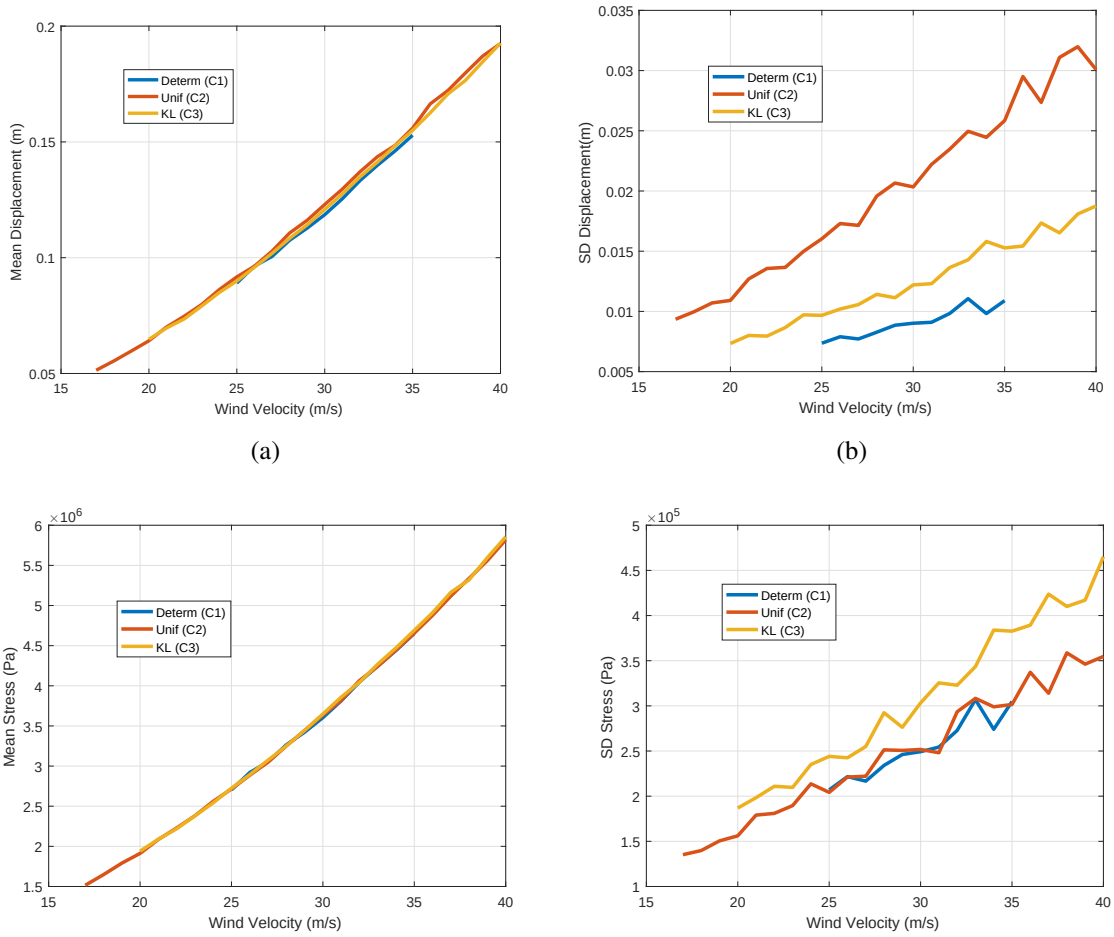

Figure 5: Top displacement of the pole and maximum bending stress at ground line. a) Mean displacements; b) SD displacements; c) mean values of normal bending stress; d) SD of normal bending stress.

a dashed line. The mode for all models is around the same value, with the largest dispersion for C2 and the smallest for C1 (as expected).

Figures 5 (a) and (b) depict the mean values and standard deviations (SD) of the top displacements as functions of the wind velocity. While the mean value for all model almost the same, the SD is larger in the C2 (Unif-model) case than in the other cases (cf. Figure 4(b-c)).The behavior observed in the C2-case can be explained as follow: the random variable MOE is assumed homogeneous along the pole and thus, the lowest (or highest) value of the MOE can be applied. In this way, the model can yield the weakest (or the strongest) pole. On the other hand, the C3 model considers zones with different values of the MOE and the probability of having the weakest (or the strongest) pole is lower than in the C2 case.

Figures 5 (c) and (d) depict the mean values and standard deviations (SD) of the bending stresses at the ground line level. In contrast to the displacement analysis, a higher SD for the KL-model is observed. The values of SD for C1 and C2 cases are almost the same. According to Euler-beam Theory, when the cross-section remains constant, the bending moment (and consequently, the normal stresses) varies with the second derivative of the product of the displacement times the MOE at each point. In cases C1 and C2, the MOE assumes a single value along the whole length, i.e. it is a constant. However, in C3 the MOE changes with the position

point to point. In cases C1 and C2 stochasticity in the stress values is due to the random nature of wind load, while in C3, the stresses are influenced by statistical origin of both the load and the material properties (MOE).

For the failure definition adopted in this work, the C2 model provides the results with more uncertainty, while C3 model offers results more closer to the deterministic MOE.

In the authors opinion, the KL-model is closer to the real case. Also, it does not differ much from the usual deterministic approach.

5 CONCLUSIONS

The structural behavior of wood utility poles under stochastic wind load and uncertain material properties was studied. Three cases were proposed for the same wind load with different MOE-models: one with deterministic mean value (C1), a second model as a random variable (C2), and a third one as a random field (C3).

Between the probabilistic material models (C2-C3), the FC derived from the C2 model is the most widespread and exhibits a wider range of failure. This FC contains more uncertainty. The FC found with the C3 model has a higher slope and exhibits failure under a smaller range of wind velocity, similar to C1 (the deterministic MOE model).

In the C2 case, the random variable MOE is assumed homogeneous along the pole and thus, the lowest (or highest) value of the MOE can be applied. In this way, the model can yield the weakest (or the strongest) pole. On the other hand, the C3 model considers zones with different values of the MOE and the probability of having the weakest (or the strongest) pole is lower than in the C2 case.

When the stress distribution at the ground line of pole is analyzed, the values of SD for C1 and C2 cases are almost the same. The MOE-model has no influence on the results, while in C3 the KL-model adds more uncertainty.

In the authors opinion, the KL-model is closer to the real case. Also, it does not differ much from the usual deterministic material approach.

REFERENCES

Ballaben J.S. and Rosales M.B. Parametric study of the dynamic along-wind response of a guyed tower. In *Proceedings of Segundo Congreso Latinoamericano de Ingeniería del Viento (CLIV2), La Plata, Argentina*. 2012.

Castro H., De Bortoli M., Paz R., and Marighetti J. Una metodología de cálculo para la determinación de la respuesta dinámica longitudinal de estructuras altas bajo la acción del viento. *Revista Internacional de Métodos Numéricos para Cálculo y Diseño en Ingeniería*, 31(4):235–245, 2015.

CIRSOC 102. *Reglamento Argentino de Acción del Viento sobre las Construcciones*. CIRSOC, 2005.

CIRSOC 601. *Proyecto de Reglamento Argentino de Estructuras de Madera CIRSOC 601*. INTI-CIRSOC, 2011.

Dyrbye C. and Hansen S.O. *Wind loads on structures*. John Wiley & Sons, 1996.

FlexPDE, PDE. Solutions inc. http://www. pdesolutions. com, 2014.

García D.A., Sampaio R., and Rosales M.B. Vibrational problems of timber beams with knots considering uncertainties. *Journal of the Brazilian Society of Mechanical Sciences and Engineering*, pages 1–13, 2015.

Mulani S.B. *Uncertainty Quantification in Dynamic Problems With Large Uncertainties*. Ph.D. thesis, Virginia Tech, 2006.

Palencia A.J.G., Saffar A., and Godoy L.A. Curvas de fragilidad debidas a viento para edificaciones industriales metalicas. *Revista Internacional de Desastres Naturales, Accidentes e Infraestructura Civil*, 8(2), 2008.

Piter J., Zerbino R., and Blaß H. Visual strength grading of argentinean eucalyptus grandis. *Holz als Roh-und Werkstoff*, 62(1):1–8, 2004.

Shannon C.E. A mathematical theory of communication. *Bell Sysmem Technical Journal*, 3(27):279–423, 1948.

Shinozuka M. and Deodatis G. Simulation of stochastic processes by spectral representation. *Applied Mechanics Reviews*, 44(4):191–204, 1991.

Torrán E., Zitto S., Cotrina A., and Piter J.C. Bending strength and stiffness of poles of argentinean eucalyptus grandis. *Maderas. Ciencia y tecnología*, 11(1):71–84, 2009.